J. of Electromagn. Waves and Appl., Vol. 25, 879–888, 2011

CFS-PML IMPLEMENTATION FOR THE UNCONDITIONALLY STABLE FDLTD METHOD

R. Mirzavand, A. Abdipour, and G. Moradi

E. E. Department, Amirkabir University of Technology
Tehran 15914, Iran

M. Movahhedi

E. E. Department, Shahid Bahonar University of Kerman
Kerman, 22 Bahman Bolv., Iran

Abstract—This paper introduces the implementation of complex frequency shifted perfectly matched layer (CFS-PML) absorbing boundary conditions for the unconditionally stable finite-difference Laguerre time-domain (FDLTD) method. It has been shown that the relative performance of the CFS-PML implementations is superior to the PML and Mur ABCs performance by an example.

1. INTRODUCTION

The FDTD method [1] is a well-known full-wave simulation methods in the microwave and antenna engineering [2–7] but has a limitation because of conditionally stability. On the other hand, the numerical dispersion error of commonly unconditionally stable methods, such as ADI-FDTD, Crank-Nicolson, and LOD-FDTD methods [8–12], becomes bigger as the time step increases [13]. Recently, a new unconditionally stable scheme for the simulation of Maxwell's equations was introduced based on the Laguerre polynomials [14]. This method is a marching-on-in-degree method instead of marching-on-in-time method. Therefore, the stability is no longer affected by the time step size [14–16]. The time step is used only to calculate the Laguerre expansion coefficients of sources done only at the start of the computations. Hence selecting a smaller value for Δt can improve the accuracy of solution to a desired value without significant

Received 8 December 2010, Accepted 14 January 2011, Scheduled 26 January 2011
Corresponding author: Abdolali Abdipour (abdipour@aut.ac.ir).

additional computation load. Therefore, Laguerre based method may be computationally much more efficient than the FDTD methods [14]. All of the previous published papers have implemented the PML or UPML for FDLTD method [17–19]. In this paper, we introduce the CFS-PML implementation for FDLTD which improves attenuation of evanescent waves and compare different ABCs in the FDTD and FDLTD implementations.

2. LAGUERRE TRANSFORM

Laguerre polynomials are defined by the Rodrigues formula [20],

$$L_p(t) = \frac{e^t}{p!}\frac{d^p}{dt^p}\left(e^t t^p\right); \quad p = 0, 1, \ldots \tag{1}$$

and the weighted Laguerre functions [15], $\psi_p(t) = e^{-t/2}L_p(t)$ are orthogonal to each other over $[0,\infty)$, i.e.,

$$\int_0^\infty \psi_p(t)\psi_q(t)dt = \begin{cases} 0 & p \neq q \\ 1 & p = q \end{cases} \tag{2}$$

which form a complete orthonormal polynomial system in the Hilbert space $L^2[0,\infty) = \left\{u : \mathcal{C} \to \mathcal{C} \,\middle|\, \|u\|^2 = \int_0^\infty e^{-t}\,|u(t)|^2 dt < \infty\right\}$ [21]. Therefore, an approximation of a function $u(\mathbf{r}, t)$ with a linear combination of modified Laguerre functions,

$$u(\mathbf{r}, t) = \sum\nolimits_{p=0}^{N} u^p(\mathbf{r})\psi_p\left(\bar{t}\right); \quad \bar{t} = s \cdot t \tag{3}$$

converges in $L^2[0,\infty)$, if $\|u\|^2 = \sum_{p=0}^{N} |u_p|^2 < \infty$. In the above equation, $\mathbf{r}= x\mathbf{a}_x+y\mathbf{a}_y+z\mathbf{a}_z$ is the position vector; s is a scaling factor to increase the time scale to the order of second; and $u^p(\mathbf{r})$ are the spatial domain expansion coefficients obtained using the orthonormal property of basis functions as,

$$u^p(\mathbf{r}) = \int_0^\infty \psi_p(\bar{t})u(\mathbf{r}, \bar{t})d\bar{t} \tag{4}$$

As $\psi_p(\bar{t}) = e^{-st/2}L_p(\bar{t})$, we have

$$\partial_t\psi_p(\bar{t}) = -0.5se^{-\bar{t}/2}L_p(\bar{t}) + se^{-\bar{t}/2}\partial_{\bar{t}}L_p(\bar{t}) \tag{5}$$

and the recursive relation $L_p(t) = \partial_t L_p(t) - \partial_t L_{p+1}(t)$ [20] leads to $\partial_t L_p(t) = \sum_{k=0}^{p-1} L_k(t)$. Therefore, the first-order partial derivative of

$u(\mathbf{r}, t)$, with respect to the time, can be expressed as,

$$\partial_t u(\mathbf{r}, t) = s \sum_{p=0}^{N} \left[0.5u^p(\mathbf{r}) + \sum_{k=0}^{p-1\geq 0} u^k(\mathbf{r}) \right] \psi_p(\bar{t}) = s \sum_{p=0}^{N} u^{pp}(\mathbf{r}) \psi_p(\bar{t}) \quad (6)$$

3. MAXWELL'S EQUATIONS IN THE LAGUERRE DOMAIN

Maxwell's equations characterize electromagnetic wave propagation completely, which can be written in a matrix form as,

$$\partial_t W = (A - B)W + J. \quad (7)$$

where $W = [E_x, E_y, E_z, H_x, H_y, H_z]^T$, $J = [J_x, J_y, J_z, 0, 0, 0]^T$, and

$$A = \begin{bmatrix} \mathbf{0} & A_1/2\varepsilon \\ A_2/2\mu & \mathbf{0} \end{bmatrix}, B = \begin{bmatrix} \mathbf{0} & A_2/2\varepsilon \\ A_1/2\mu & \mathbf{0} \end{bmatrix};$$

$$A_1 = \begin{bmatrix} 0 & 0 & \partial_y \\ \partial_z & 0 & 0 \\ 0 & \partial_x & 0 \end{bmatrix}, \quad A_2 = \begin{bmatrix} 0 & \partial_z & 0 \\ 0 & 0 & \partial_x \\ \partial_y & 0 & 0 \end{bmatrix} \quad (8)$$

In the above equations, E is the electric field; H is the magnetic field; J is the total current density; ε and μ are the electric permittivity and the magnetic permeability, respectively. According to (3), the approximation of components of (8) can be expanded as,

$$W(\mathbf{r}, t) = \sum_{p=0}^{\infty} w^p(\mathbf{r}) \psi_p(\bar{t}) \quad \text{and} \quad J(\mathbf{r}, t) = \sum_{p=0}^{\infty} J^p(\mathbf{r}) \psi_p(\bar{t}) \quad (9)$$

where $w^p = [e_x^p, e_y^p, e_z^p, h_x^p, h_y^p, h_z^p]$ and $J^p = [j_x^p, j_y^p, j_z^p, 0, 0, 0]$ are unknown coefficients. Substituting (9) into (7) and using (6), Laguerre domain Maxwell's equations are obtained as,

$$s \sum_{p=0}^{N} w^{pp}(\mathbf{r}) \psi_p(\bar{t}) = \sum_{p=0}^{N} (A - B) w^p(\mathbf{r}) \psi_p(\bar{t}) + \sum_{p=0}^{N} J^p(\mathbf{r}) \psi_p(\bar{t}) \quad (10)$$

Multiplying both sides of (10) by $\psi_m(\bar{t})$, integrating over $\bar{t} = [0, \infty)$ and using (2), we get a set of $(N + 1)$ boundary value problems as,

$$s w^{mm}(\mathbf{r}) = (A - B) w^m(\mathbf{r}) + J^m(\mathbf{r}); \quad m = 0, 1, \ldots N \quad (11)$$

Using Yee's space lattice [1] and the central difference scheme for spatial derivatives for A and B, (11) is discretized for the numerical simulation. For example, e_x and h_x have the following relations,

$$\begin{aligned} & e^m_{x|i,j,k} - a_y\left(h^m_{z|i,j,k} - h^m_{z|i,j-1,k}\right) - a_z\left(h^m_{y|i,j,k} - h^m_{y|i,j,k-1}\right) \\ = & \frac{2}{s} j^m_{x|i,j,k} - 2\sum_{d=0}^{m-1} e^d_{x|i,j,k} \end{aligned} \tag{12}$$

$$\begin{aligned} & h^m_{x|i,j,k} - b_z\left(e^m_{y|i,j,k+1} - e^m_{y|i,j,k}\right) - b_y\left(e^m_{z|i,j+1,k} + e^m_{z|i,j,k}\right) \\ = & -2\sum_{d=0}^{m-1} h^d_{x|i,j,k} \end{aligned} \tag{13}$$

while $(i,j,k) \in (1 : N_x, 1 : N_y, 1 : N_z)$, $a_\vartheta = 1/\varepsilon s \Delta\vartheta$ and $b_\vartheta = 1/\mu s \Delta\vartheta$.

4. CFS-PML ABSORBING BOUNDARY CONDITION FOR THE FDLTD

The frequency domain PML equation for E_x in the stretched coordinates is given by [22]

$$j\omega\varepsilon E_x = s_y^{-1}\partial_y H_z - s_z^{-1}\partial_z H_y \tag{14}$$

The stretched co-ordinate variable [23] $s_\vartheta = \kappa_\vartheta + \sigma_\vartheta/(\alpha_\vartheta + j\omega\varepsilon_0)$ is defined for $\vartheta \in (x, y, z)$ while α_ϑ and σ_ϑ are assumed to be positive real, and κ_ϑ is real and greater than 1. Considering frequency dependence of the stretched coordinate metrics, the time domain transformation of (14) has convolutions in the right-hand-side as [22]

$$\varepsilon\partial_t E_x = \bar{s}_y(t) * \partial_y H_z - \bar{s}_z(t) * \partial_z H_y \tag{15}$$

where $\bar{s}_\vartheta$ is the inverse Laplace transform of s_ϑ^{-1} and

$$\bar{s}_\vartheta(t) = \frac{\delta(t)}{\kappa_\vartheta} - \frac{\sigma_\vartheta u(t)}{\varepsilon_0\kappa_\vartheta^2} e^{-\left(\frac{\sigma_\vartheta+\kappa_\vartheta\alpha_\vartheta}{\varepsilon_0\kappa_\vartheta}\right)t} = \frac{\delta(t)}{\kappa_\vartheta} - \frac{\sigma_\vartheta u(t)}{\varepsilon_0\kappa_\vartheta^2} e^{-\gamma_\vartheta t}. \tag{16}$$

Using $\psi_m * \psi_n = \psi_{m+n} - \psi_{m+n+1}$ [20], the relation of a^p, b^p, and c^p as the expansion coefficients of the convolution relation $A = B * C$ in the Laguerre domain is given by,

$$\sum_{p=0}^{N} a^p\psi_p = \sum_{m=0}^{N} b^m\psi_m * \sum_{n=0}^{N} c^n\psi_n = \sum_{m=0}^{N}\sum_{n=0}^{N} b^m c^n\left(\psi_{m+n} - \psi_{m+n+1}\right) \tag{17}$$

If the left-hand-side and right-hand-side of (17) are compared on a term-by-term Laguerre order, the following equation can be obtained,

$$a^p = b^p c^0 + \sum_{k=0}^{p-1} b^k\left(c^{p-k} - c^{p-k-1}\right) \tag{18}$$

Using (4), the expansion coefficients of the exponential function $e^{-\gamma_\vartheta t}$ in (16) is calculated analytically as $(\gamma_\vartheta)^p/(\gamma_\vartheta+1)^{p+1}$. Therefore, (15) is transformed to the Laguerre domain as,

$$\begin{aligned}
& e^m_{x|i,j,k} - c_y\left(h^m_{z|i,j,k} - h^m_{z|i,j-1,k}\right) + c_z\left(h^m_{y|i,j,k} - h^m_{y|i,j,k-1}\right) \\
&= -\sum_{p=0}^{m-1}\left(D^p_{hzy}S^{m-p}_y - D^p_{hyz}S^{m-p}_z + 2e^p_{x|i,j,k}\right); \\
c_\vartheta &= \frac{2(\sigma_\vartheta - \varepsilon_0\kappa_\vartheta)}{s\varepsilon_0\varepsilon\kappa^2_\vartheta\Delta\vartheta}, \qquad S^m_\vartheta = \frac{-\sigma_\vartheta(\gamma_\vartheta)^m}{\varepsilon_0\kappa^2_\vartheta(\gamma_\vartheta+1)^{m+1}}, \\
\mathcal{D}^m_{hzy} &= \frac{h^m_{z|i,j,k} - h^m_{z|i,j-1,k}}{0.5\varepsilon s\Delta y_j}, \quad \mathcal{D}^m_{hyz} = \frac{h^m_{y|i,j,k} - h^m_{y|i,j,k-1}}{0.5\varepsilon s\Delta z_k}
\end{aligned} \tag{19}$$

Defining $d_\vartheta = \varepsilon c_\vartheta/\mu$, the equation for h_x is obtained similarly as,

$$\begin{aligned}
& h^m_{x|i,j,k} - d_z\left(e^m_{y|i,j,k+1} - e^m_{y|i,j,k}\right) + d_y\left(e^m_{z|i,j+1,k} - e^m_{z|i,j,k}\right) \\
&= -\sum_{p=0}^{m-1}\left(D^p_{eyz}S^{m-p}_z - D^p_{ezy}S^{m-p}_y + 2h^p_{x|i,j,k}\right); \\
\mathcal{D}^m_{ezy} &= \frac{e^m_{z|i,j+1,k} - e^m_{z|i,j,k}}{0.5\mu s\Delta y_j}, \mathcal{D}^m_{eyz} = \frac{e^m_{y|i,j,k+1} - e^m_{y|i,j,k}}{0.5\mu s\Delta z_k}
\end{aligned} \tag{20}$$

The other PML equations are written similarly. It is significant that (12) and (13) in the main region and (19) and (20) in the PML region have similar forms. To reduce the required simulation memory and computation time, we can eliminate the unknown magnetic field components from (12) and (19), using equations for h_y and h_z. For example, (12) can be written as,

$$\begin{aligned}
&(1+2a_yb_y+2a_zb_z)\,e^m_{x|i,j,k} - a_yb_y\left(e^m_{x|i,j+1,k} + e^m_{x|i,j-1,k}\right) \\
&-a_zb_z\left(e^m_{x|i,j,k+1} + e^m_{x|i,j,k-1}\right) \\
&+a_yb_x\left(e^m_{y|i+1,j,k} - e^m_{y|i,j,k} - e^m_{y|i+1,j-1,k} + e^m_{y|i,j-1,k}\right) \\
&+a_zb_x\left(e^m_{z|i+1,j,k} - e^m_{z|i,j,k} - e^m_{z|i+1,j,k-1} + e^m_{z|i,j,k-1}\right) = \frac{2}{s}j^m_{x|i,j,k} - \\
&2\sum_{d=0}^{m-1}\left(e^d_{x|i,j,k} + a_yh^d_{z|i,j,k} - a_yh^d_{z|i,j-1,k} - a_zh^d_{y|i,j,k} + a_zh^d_{y|i,j,k-1}\right)
\end{aligned} \tag{21}$$

Consequently, the implicit relations for the electric fields can be written in the matrix form of,

$$Ce^m = j^m + \sum_{d=0,m\neq 0}^{m-1} f\left(e^d, h^d\right); \quad m = 0, 1, \dots N \tag{22}$$

where $e^m = [e_x^m e_y^m e_z^m]^T$, $j^m = [j_x^m j_y^m j_z^m]^T$, $h^m = [h_x^m h_y^m h_z^m]^T$, and f is a linear function of e^d and h^d. The coefficient matrix C in (22) is a constant matrix with respect to m. Therefore, we need to perform the matrix inversion only once at the beginning of the computation. Starting from $m = 0$ and using calculated coefficients of current source j^m by (4), the right-hand-side of (22) is known, and the unknown coefficients e^m can be calculated recursively for $m > 0$. Then, the magnetic field coefficients can be obtained from (13) and (20). Finally, the values of fields in the time domain are calculated from the above coefficients and (3).

5. NUMERICAL RESULTS

In order to evaluate the presented boundary condition, a simple experiment was undertaken. The testing procedure is a $2D$ example containing two cartesian grids. The testing procedure is a 2D example containing two cartesian grids: A small 50×50 cells grid which is truncated by different numerical absorbers and a large 250×250 cells grids with an arbitrary boundary condition, as shown in Fig. 1. The model was constructed with a hard sinusoid source in the middle of the grids. The source was set to have a wavelength of 1, and the FDTD grids have a distance of $\Delta_x = 0.05$, satisfying the $\lambda/20$ sampling required for high-quality finite difference results. Considering routes L_1 and L_2 and domains D_1 and D_2 in Fig. 1, the simulation time was set so that the reflections from the ABC under test (L_2) propagate back to the observation point, but any back reflections generated by the boundary of computational domain (L_1) would not have sufficient time to propagate back to the observation point. Therefore, the field values collected with D_2 have the adverse effects of back reflections from the ABCs present in them, while the field values collected with D_1 have not been affected by any back reflections.

The error introduced by the absorbing boundary condition is determined by calculating the Root-Mean Square (RMS) error between the field value in D_1 and the corresponding point in D_2 for every time step. Fig. 2 shows the normalized magnitude of electric field respect to the magnitude of source in an example observation point $(10, 10)$ calculated by FDTD and FDLTD methods. The results are

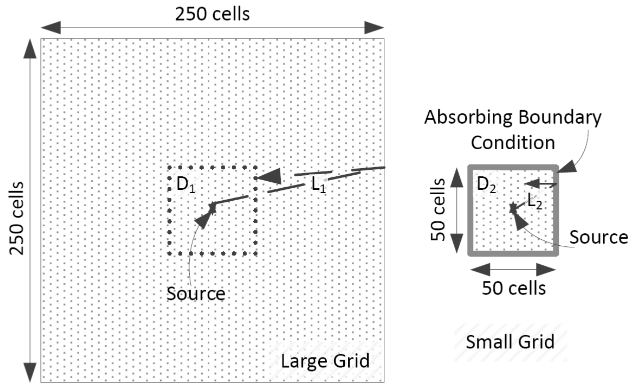

Figure 1. Geometry for the calculation of the error introduced by different absorbing boundary conditions.

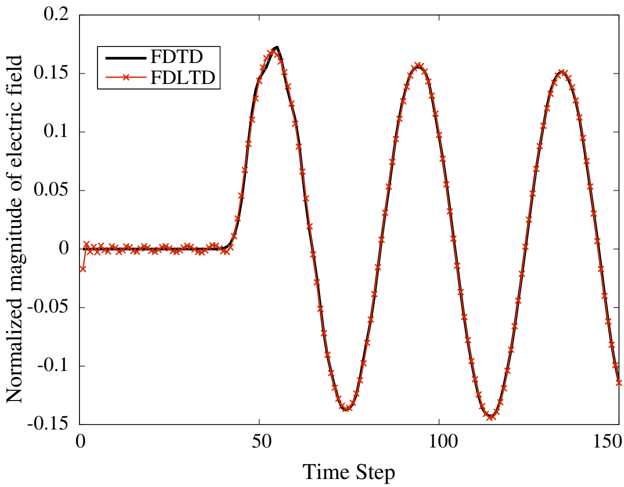

Figure 2. Normalized magnitude of electric field in an example observation point calculated by FDTD and FDLTD methods.

very close to each other, while the FDLTD is 10 times faster than the FDTD in this example. Fig. 3 shows the RMS error of FDTD and FDLTD implementations with 2nd order Mur, PML (which is equivalent to the CFS-PML with $\alpha = 0$) with 8 and PML with 16 layers, and CFS-PML with 4 layers as absorbing boundary condition. Each boundary condition gives approximately the same accuracy for FDTD and FDLTD methods. As can be seen, CFS-PML with only

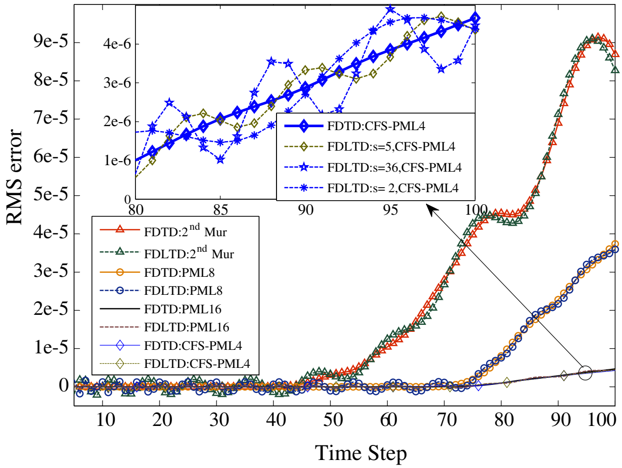

Figure 3. Comparisons between the Mur, PML and CFS-PML ABCs in the FDTD and FDLTD implementations.

4 layers works similarly to PML with 16 layers and is superior to the other ABCs. The FDLTD simulation contains 100 modified Laguerre functions. Simulation results show that the error of approximation is minimal for $5 \leq s \leq 35$ (Fig. 3). The profile of the PML parameters is determined similar to [22] as $\alpha = 0.05$, $\kappa_{\max} = 11.0$, and $\sigma_{\max} = 0.7/30\pi\sqrt{\varepsilon_r}\Delta_x$ with a 4th order polynomial scaling.

6. CONCLUSION

We have proposed a new CFS-PML implementation for the unconditionally stable FDLTD method which can also implement PML when $\alpha = 0$. Simulation results show that CFS-PML with only 4 layers works similarly to PML with 16 layers and is superior to Mur ABC.

ACKNOWLEDGMENT

This work was supported in part by the Education and Research Institute for ICT (ERICT).

REFERENCES

1. Yee, K. S., "Numerical solution of initial boundary value problems involving Maxwells equations in isotropic media," *IEEE*

Transactions on Antennas and Propagation, Vol. 14, 302–307, 1966.

2. Zhang, Y.-Q. and D.-B. Ge, "A unified FDTD approach for electromagnetic analysis of dispersive objects," *Progress In Electromagnetics Research*, Vol. 96, 155–172, 2009.
3. Dai, S. Y., C. M. Zhang, and Z. S. Wu, "Electromagnetic scattering of objects above ground using MRTD/FDTD hybrid method," *Journal of Electromagnetic Waves and Applications*, Vol. 23, No. 16, 2187–2196, 2009.
4. Li, J., L.-X. Guo, and H. Zeng, "FDTD method investigation on the polarimetric scattering from 2-D rough surface," *Progress In Electromagnetics Research*, Vol. 101, 173–188, 2010.
5. Xiao, S.-Q., Z. Shao, and B.-Z. Wang, "Application of the improved matrix type FDTD method for active antenna analysis," *Progress In Electromagnetics Research*, Vol. 100, 245–263, 2010.
6. Yang, S., Y. Chen, and Z.-P. Nie, "Simulation of time modulated linear antenna arrays using the FDTD method," *Progress In Electromagnetics Research*, Vol. 98, 175–190, 2009.
7. Chen, C. Y., Q. Wu, X. J. Bi, Y. M. Wu, and L. W. Li, "Characteristic analysis for FDTD based on frequency response," *Journal of Electromagnetic Waves and Applications*, Vol. 24, No. 2–3, 283–292, 2010.
8. Zheng, F., Z. Chen, and J. Zhang, "A finite-difference time-domain method without the Courant stability conditions," *IEEE Microwave and Guided Wave Letters*, Vol. 9, No. 11, 441–443, 1999.
9. Ahmed, I., E. K. Chua, E. P. Li, and Z. Chen, "Development of the three dimensional unconditionally stable LODFDTD method," *IEEE Transactions on Antennas and Propagation*, Vol. 56, No. 11, 3596–3600, 2008.
10. Rouf, H. K., F. Costen, S. G. Garcia, and S. Fujino, "On the solution of 3-D frequency dependent Crank-Nicolson FDTD scheme," *Journal of Electromagnetic Waves and Applications*, Vol. 23, No. 16, 2163–2175, 2009.
11. Tay, W. C. and E. L. Tan, "Implementations of PMC and PEC boundary conditions for efficient fundamental ADI- and LOD-FDTD," *Journal of Electromagnetic Waves and Applications*, Vol.24, No. 4, 565–573, 2010.
12. Xu, K., Z. Fan, D.-Z. Ding, and R.-S. Chen, "Gpu accelerated unconditionally stable Crank-Nicolson FDTD method for the analysis of three-dimensional microwave circuits," *Progress In*

Electromagnetics Research, Vol. 102, 381–395, 2010.

13. Kong, K. B., S. O. Park, and J. S. Kim, "Stability and numerical dispersion of 3-D simplified sampling biorthogonal ADI method," *Journal of Electromagnetic Waves and Applications*, Vol. 24, No. 1, 1–12, 2010.
14. Chung, Y. S., T. K. Sarkar, B. H. Jung, and M. Salazar-Palma, "An unconditionally stable scheme for the finite-difference time-domain method," *IEEE Transactions on Microwave Theory and Techniques*, Vol. 51, No. 3, 697–704, 2003.
15. Zhao, H. and Z. Shen, "Weighted laguerre polynomials-finite difference method for time-domain modeling of thin wire antennas in a loaded cavity," *IEEE Antennas and Wireless Propagation Letters*, Vol. 8, 1131–1134, 2009.
16. Lin, H., G. Wang, and F. Liang, "A novel unconditionally stable PSTD method based on weighted laguerre polynomial expansion," *Journal of Electromagnetic Waves and Applications*, Vol. 23, No. 8–9, 1011–1020, 2009.
17. Liang, F., H. Lin, and G. Wang, "An unconditionally stable wave equation PML algorithm for truncating FDTD simulation," *Microwave and Optical Technology Letters*, Vol. 51, No. 4, 1028–1032, 2009.
18. Duan, Y. T., B. Chen, H. L. Chen, and Y. Yi, "Anisotropic-medium PML for efficient Laguerre-based FDTD method," *Electronc Letters*, Vol. 46, No. 5, 2010.
19. Ding, P. P., G. Wang, H. Lin, and B. Z. Wang, "Unconditionally stable FDTD formulation with UPML-ABC," *IEEE Microwave and Wireless Components Letters*, Vol. 16, No. 4, 161–163, 2006.
20. Gradshteyn, I. S. and I. M. Ryzhik, *Table of Integrals, Series, and Products*, Academic, New York, 1980.
21. Weniger, E. J., "On the analyticity of laguerre series," *Journal of Physics A: Mathematical and Theoretical*, Vol. 41, No. 42, 425207-1–425207-43, 2008.
22. Roden, J. A. and S. D. Gedney, "Convolution PML (CPML): An efficient FDTD implementation of the CFSPML for arbitrary media," *Microwave and Optical Technology Letters*, Vol. 27, No. 5, 334–339, 2000.
23. Berenger, J. P., "A perfectly matched layer for the absorption of electromagnetic waves," *Journal of Computational Physics*, Vol. 114, No. 2, 185–200, 1994.